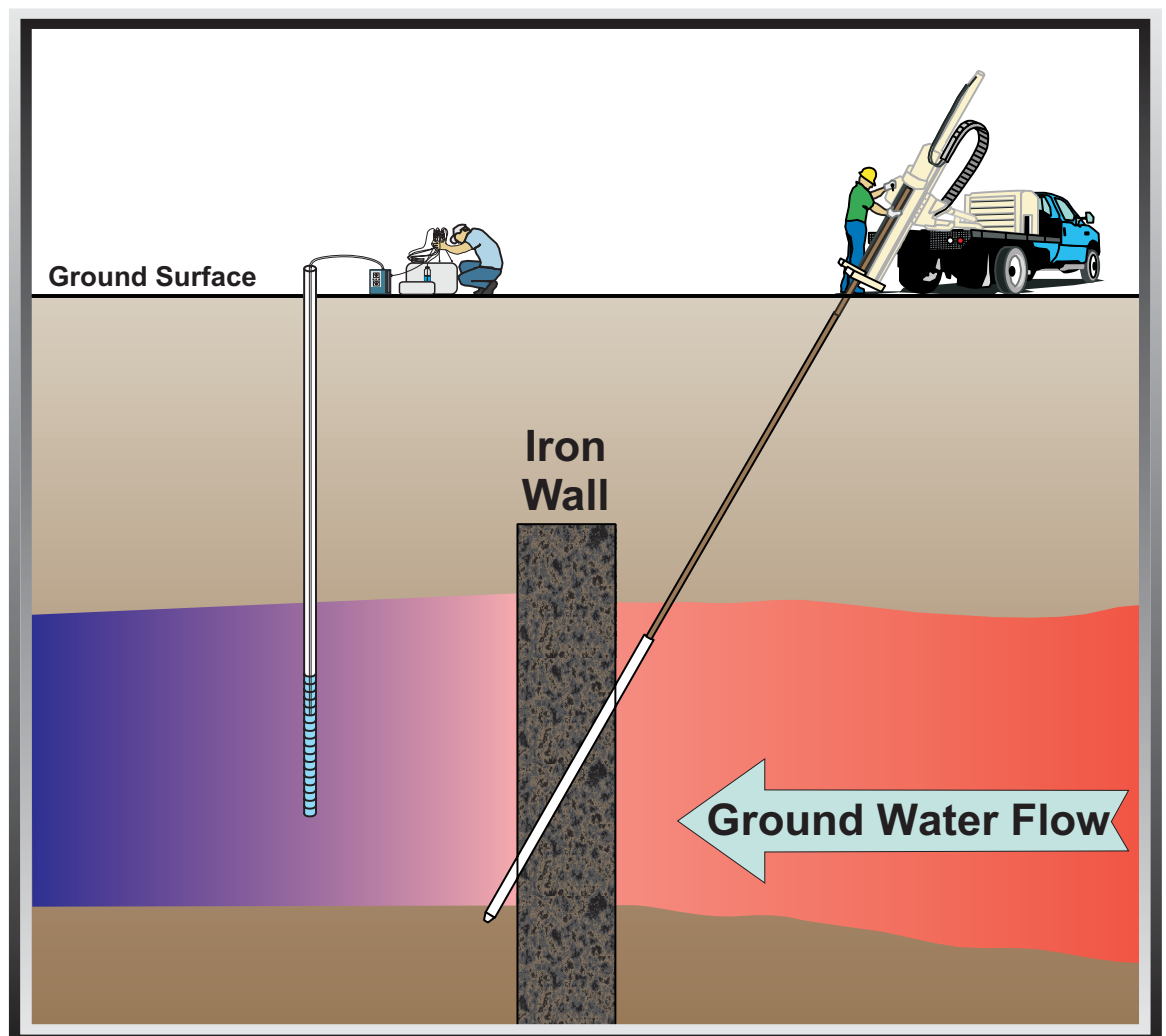


Capstone Report on the Application, Monitoring, and Performance of Permeable Reactive Barriers for Ground-Water Remediation:

Volume 1

Performance Evaluations at Two Sites



Capstone Report on the Application, Monitoring, and Performance of Permeable Reactive Barriers for Ground-Water Remediation:

Volume 1 – Performance Evaluations at Two Sites

Richard T. Wilkin and Robert W. Puls
Ground Water and Ecosystems Restoration Division
National Risk Management Research Laboratory
Ada, Oklahoma 74820

National Risk Management Research Laboratory
Office of Research and Development
U.S. Environmental Protection Agency
Cincinnati, OH 45268

Notice

The U.S. Environmental Protection Agency through its Office of Research and Development funded the research described here. It has been subjected to the Agency's peer and administrative review and has been approved for publication as an EPA document. Mention of trade names or commercial products does not constitute endorsement or recommendation for use.

All research projects making conclusions or recommendations based on environmentally related measurements and funded by the Environmental Protection Agency are required to participate in the Agency Quality Assurance Program. This project was conducted under an approved Quality Assurance Project Plan. The procedures specified in this plan were used without exception. Information on the plan and documentation of the quality assurance activities and results are available from the Principal Investigator.

Foreword

The U.S. Environmental Protection Agency (EPA) is charged by Congress with protecting the Nation's land, air, and water resources. Under a mandate of national environmental laws, the Agency strives to formulate and implement actions leading to a compatible balance between human activities and the ability of natural systems to support and nurture life. To meet this mandate, EPA's research program is providing data and technical support for solving environmental problems today and building a science knowledge base necessary to manage our ecological resources wisely, understand how pollutants affect our health, and prevent or reduce environmental risks in the future.

The National Risk Management Research Laboratory (NRMRL) is the Agency's center for investigation of technological and management approaches for preventing and reducing risks from pollution that threatens human health and the environment. The focus of the Laboratory's research program is on methods and their cost-effectiveness for prevention and control of pollution to air, land, water, and subsurface resources; protection of water quality in public water systems; remediation of contaminated sites, sediments and ground water; prevention and control of indoor air pollution; and restoration of ecosystems. NRMRL collaborates with both public and private sector partners to foster technologies that reduce the cost of compliance and to anticipate emerging problems. NRMRL's research provides solutions to environmental problems by: developing and promoting technologies that protect and improve the environment; advancing scientific and engineering information to support regulatory and policy decisions; and providing the technical support and information transfer to ensure implementation of environmental regulations and strategies at the national, state, and community levels.

This publication has been produced as part of the Laboratory's strategic long-term research plan. It is published and made available by EPA's Office of Research and Development (ORD) to assist the user community and to link researchers with their clients. The purpose of this document is to provide detailed performance monitoring data on full-scale Permeable Reactive Barriers (PRBs) installed to treat contaminated ground water at two different sites. This report will fill a need for a readily available source of information for site managers and others who are faced with the need to remediate ground water contaminated by chlorinated solvents, chromium, arsenic, nitrates, and other organic and inorganic compounds and are considering the use of this cost-effective technology. The PRBs discussed in this report are among the oldest full-scale systems available for study and provide an opportunity to analyze the performance of systems with more than five years of field history. In addition, the PRBs examined here have contrasting design and hydrogeochemical characteristics that are useful in the context of gaining insight about the factors that govern PRB longevity and long-term performance. The information provided in this document will be of use to stakeholders such as state and federal regulators, Native American tribes, consultants, contractors, and other interested parties.



Ground Water and Ecosystems Restoration Division
National Risk Management Research Laboratory

Abstract

Research results discussed in this report explore the geochemical and microbiological processes within zero-valent iron Permeable Reactive Barriers (PRBs) that may contribute to changes through time in iron reactivity and decreases in reaction zone permeability. Two full-scale PRBs were evaluated in this study: the U.S. Coast Guard Support Center PRB located near Elizabeth City, North Carolina, and the Denver Federal Center PRB in Lakewood, Colorado. Detailed water sampling and analysis, core sampling, and solid-phase characterization studies were carried out to: i) evaluate spatial and temporal trends in contaminant concentrations and key geochemical parameters; ii) characterize the type and nature of surface precipitates forming over time in the reactive barriers; and iii), identify the type and extent of microbiological activity within and around the reactive barriers.

Trends in geochemical parameters (e.g., pH and oxidation-reduction potential) may signal changes in system performance, but no clear correlations between these parameters and decreased system performance have been observed to date at the sites studied. Long-term trends in geochemical parameters are consistent with contaminant removal trends observed at both sites. Spatial and temporal variations in the concentration distribution of terminal electron accepting species (e.g., sulfate), specific conductance, and Eh suggest that both anaerobic iron corrosion and microbial activity play important roles in controlling the oxidation-reduction potential in iron barriers. Low Eh values (≤ 100 mV relative to the standard hydrogen electrode) and decreases in the specific conductance of ground water between upgradient contaminant plumes and sampling points within reactive iron media are consistently observed in normally operating PRB systems.

The rate of mineral and biomass buildup was evaluated at both sites. The principal factors that determine the amount of mineral precipitation in zero-valent iron PRBs are flow rate, ground-water chemistry, and microbial activity. After five years of operation, the Elizabeth City and Denver Federal Center reactive barriers have developed consistent patterns of spatially variable mineral precipitation and microbial activity. The development of precipitation and biomass fronts result from abrupt geochemical changes that occur at upgradient interface regions coupled with ground water solute transport. Upgradient regions at both sites investigated in this study have witnessed the greatest accumulation of mineral mass and biomass. However, neither of the sites of this study show complete filling of available pore space after five years, suggesting that flow characteristics should not be affected by the accumulation of authigenic components. For zero-valent iron systems, the reactive media is a long-term sink for C, S, Ca, Si, Mg, and N. Porosity loss in the iron media due to precipitation of inorganic carbon and sulfur minerals can be estimated by integrating the concentrations of inorganic carbon and sulfur as a function of distance in the iron and estimating the volume loss by using the molar volumes of zero-valent iron, calcium carbonate, iron carbonate, and iron sulfide. Porosity loss estimates have ranged from about 1% to 4% per year in this study. Based on these estimates, the average porosity of the PRB at Elizabeth City, for example, would not be expected to approach that of the surrounding aquifer for 15 to 30 years. As corrosion minerals form on the surface of the iron media, reactive surfaces are coated, presumably decreasing the effective reactive surface area. However, corrosion products formed include some minerals which themselves are highly reactive and capable of transforming inorganic and organic contaminants into immobile or non-toxic forms. This phenomenon must also be factored into lifetime projections.

While long-term performance observations of the Elizabeth City and Denver Federal Center site are now past five years, there has still not been sufficient time to adequately predict the lifetime of these PRBs or most other PRBs. It is clear that lifetimes exceeding 10 years are reasonable to expect under some conditions and that PRBs may function adequately for much longer. Continued studies are needed to better predict longevity based on ground-water composition, flow rate and contaminant flux.

Table of Contents

Notice	ii
Foreword	iii
Abstract	iv
Table of Contents	v
Figures	vii
Tables	xii
Acknowledgments	xiv
1.0 Introduction	1
1.1 Federal Tri-Agency Initiative	2
1.1.1 DoD Studies	2
1.1.2 DOE Studies	3
1.1.3 EPA Studies	3
2.0 Site Descriptions	5
2.1 U.S. Coast Guard Support Center	5
2.2 Denver Federal Center	5
3.0 Elizabeth City PRB Monitoring Results	9
3.1 Ground Water Monitoring	9
3.1.1 Contaminant Behavior	9
3.1.2 Geochemical Parameters	13
3.1.3 Dissolved Cations and Anions	18
3.2 Core Sampling at Elizabeth City	25
3.2.1 Carbon Analysis	25
3.2.2 Sulfur Analysis	33
3.2.3 Cr Extractions	39
3.2.4 X-ray Diffraction Analysis	39
3.2.5 Scanning Electron Microscopy	41
3.2.6 Microbial Characterization	46
3.3 Summary of Results from the Elizabeth City Site	52
4.0 Denver Federal Center Monitoring Results	53
4.1 Ground Water Monitoring	53
4.1.1 Gate 1 Contaminant Behavior	53
4.1.2 Gate 2 Contaminant Behavior	58
4.1.3 Gate 3 Contaminant Behavior	58
4.1.4 Geochemical Parameters	58
4.1.5 Hydrogen Gas Concentrations	62
4.1.6 Dissolved Cations and Anions	64
4.2 Core Sampling at the Denver Federal Center	68
4.2.1 Carbon Analysis	71
4.2.2 Sulfur Analysis	71
4.2.3 X-ray Diffraction Analysis	71
4.2.4 Scanning Electron Microscopy	71
4.2.5 Microbial Characterization	80
4.3 Summary of Results from the Denver Federal Center Site	82

5.0 Factors Affecting Longevity and Performance	87
5.1 Fe ⁰ Dissolution	87
5.2 Anion Composition	89
5.2.1 Bicarbonate Reactions	89
5.2.2 Sulfate Reactions	96
5.2.3 Nitrate Reactions	97
5.2.4 Reactions with Silica	97
5.2.5 Reactions with Oxygen	98
5.3 Mineral Precipitation	99
5.3.1 Pore Volume Reduction	99
5.3.2 Loss of Reactivity.	103
5.4 Microbial Activity	104
5.5 Hydrogeological Issues	107
6.0 State of Permeable Reactive Barrier Technology and Lessons Learned from Long-Term Performance Monitoring	111
6.1 Permeable Reactive Barriers: An Accepted Remedial Option for Containment & Treatment of Contaminated Ground Water	111
6.2 Lessons Learned: Site Characterization and PRB Construction	112
6.3 Lessons Learned: Long-term Performance Assessments of PRBs	112
6.3.1 Recommendations for Future Research.	113
7.0 References	115
Appendix A	121
Appendix B	135

Figures

Figure 2.1	Plan view map of the PRB at the U.S. Coast Guard Support Center, Elizabeth City, NC	7
Figure 2.2	Plan view map of the PRB at the Denver Federal Center, Lakewood, CO (after McMahon et al., 1999)	8
Figure 2.3	Schematic cross-section of the Denver Federal Center funnel-and-gate system (after McMahon et al., 1999)	8
Figure 3.1	Concentrations of contaminants through time in monitoring wells located hydraulically upgradient of the Elizabeth City PRB	10
Figure 3.2	Concentrations of TCE ($\mu\text{g/L}$) through time in monitoring wells located hydraulically downgradient of the Elizabeth City PRB	13
Figure 3.3	Cross-sectional profiles showing total chromium concentrations (mg/L) in transects 1, 2, and 3 (Elizabeth City PRB)	14
Figure 3.4	Cross-sectional profiles showing TCE concentrations ($\mu\text{g/L}$) in transects 1, 2, and 3 (Elizabeth City PRB)	15
Figure 3.5	Cross-sectional profiles showing cis-DCE concentrations ($\mu\text{g/L}$) in transects 1, 2, and 3 (Elizabeth City PRB)	16
Figure 3.6	Cross-sectional profiles showing VC concentrations ($\mu\text{g/L}$) in transects 1, 2, and 3 (Elizabeth City PRB)	17
Figure 3.7	Cross-sectional profiles showing pH distributions in transects 1, 2, and 3 (Elizabeth City PRB)	19
Figure 3.8	Cross-sectional profiles showing Eh distributions (mV) in transects 1, 2, and 3 (Elizabeth City PRB)	20
Figure 3.9	Cross-sectional profiles showing specific conductance distributions ($\mu\text{S/cm}$) in transects 1, 2, and 3 (Elizabeth City PRB)	21
Figure 3.10	Cross-sectional profiles showing calcium concentrations (mg/L) in transects 1, 2, and 3 (Elizabeth City PRB)	22
Figure 3.11	Cross-sectional profiles showing magnesium concentrations (mg/L) in transects 1, 2, and 3 (Elizabeth City PRB)	23
Figure 3.12	Cross-sectional profiles showing sodium concentrations (mg/L) in transects 1, 2, and 3 (Elizabeth City PRB)	24
Figure 3.13	Cross-sectional profiles showing potassium concentrations (mg/L) in transects 1, 2, and 3 (Elizabeth City PRB)	26
Figure 3.14	Cross-sectional profiles showing chloride concentrations (mg/L) in transects 1, 2, and 3 (Elizabeth City PRB)	28
Figure 3.15	Cross-sectional profiles showing sulfate concentrations (mg/L) in transects 1, 2, and 3 (Elizabeth City PRB)	29

Figure 3.16 Cross-sectional profiles showing alkalinity distributions (mg/L) in transects 1, 2, and 3 (Elizabeth City PRB)	30
Figure 3.17 Cross-sectional profiles showing nitrate concentrations (mg/L) in transects 1, 2, and 3 (Elizabeth City PRB)	31
Figure 3.18 Cross-sectional profiles showing silica concentrations (mg/L) in transect 2 (Elizabeth City PRB)	33
Figure 3.19 Coring locations and monitoring well locations at the Elizabeth City PRB (plan view)	34
Figure 3.20 Cross-sectional profile showing concentration distribution of inorganic carbon in the solid phase ($\mu\text{g/g}=\text{ppm}$), Elizabeth City PRB (June 2002)	36
Figure 3.21 Concentrations of inorganic carbon ($\mu\text{g/g}$) in core materials through time, Elizabeth City PRB	37
Figure 3.22 Cross-sectional profile showing concentration distribution of sulfur in the solid phase ($\mu\text{g/g}=\text{ppm}$), Elizabeth City PRB (June 2002)	38
Figure 3.23 Powder X-ray diffraction data from fine-grained materials removed via sonication from cores collected at the Elizabeth City PRB: a) core EC060300-4; b) core EC050801-3	40
Figure 3.24 Scanning electron micrographs of samples from the Elizabeth City PRB: a) sample EC060300-4-1; b) sample EC060300-4-3; c) EC060300-4-7	42-44
Figure 3.25 Iron concentration versus oxygen concentration in iron grains and surface precipitates (SEM-EDX)	46
Figure 3.26 Element concentrations in surface precipitates from the Elizabeth City PRB	48
Figure 3.27 Cross-sectional profile showing concentration distribution of biomass (from PLFA data) in picomoles per gram, Elizabeth City PRB (June 2002)	49
Figure 3.28 Histograms of microbial biomass concentrations (from PLFA data) in picomoles per gram in aquifer materials, iron from near the upgradient aquifer/iron interface, and iron from near the downgradient aquifer/iron interface	50
Figure 3.29 Pie graphs showing structural distribution of PLFA compounds (average values) at the Elizabeth City site	51
Figure 4.1 Coring locations and monitoring well locations at the Denver Federal Center, gate 1 (plan view)	54
Figure 4.2 Coring locations and monitoring well locations at the Denver Federal Center, gate 2 (plan view)	55
Figure 4.3 Coring locations and monitoring well locations at the Denver Federal Center, gate 3 (plan view)	56
Figure 4.4 Concentrations of contaminants through time in monitoring wells from the Denver Federal Center, gate 1 (data from FHWA): a) well GSA-21 (upgradient); b) well C1-11 (iron wall); c) well GSA-20 (downgradient)	57

Figure 4.5	Concentrations of contaminants through time in monitoring wells from the Denver Federal Center, gate 2 (data from FHWA): a) well GSA-26 (upgradient); b) well C2-I2 (iron wall); c) well GSA-25 (downgradient)	59
Figure 4.6	Depth-resolved concentrations of a) contaminants ($\mu\text{g/L}$) and b) sulfate, calcium, and iron (mg/L) in wells GSA-26 and GSA-25 from the Denver Federal Center (gate 2)	60
Figure 4.7	Concentrations of contaminants through time in monitoring wells from the Denver Federal Center, gate 3 (data from FHWA): a) well GSA-31 (upgradient); b) well C3-I2 (iron wall); c) well GSA-30 (downgradient)	61
Figure 4.8	Average pH values through time in wells from upgradient, iron wall, and downgradient positions relative to gate 1, gate 2, and gate 3 at the Denver Federal Center	62
Figure 4.9	Average specific conductance values ($\mu\text{S/cm}$) through time in wells from upgradient, iron wall, and downgradient positions relative to gate 1, gate 2, and gate 3 at the Denver Federal Center	63
Figure 4.10	Average Eh (V) values through time in wells from upgradient, iron wall, and downgradient positions relative to gate 1, gate 2, and gate 3 at the Denver Federal Center	63
Figure 4.11	Concentrations of dissolved hydrogen (log molar) as a function of sampling position and time in gate 1 at the Denver Federal Center. Also shown are the concentration ranges of dissolved hydrogen measured in the iron media in gate 2 and gate 3	64
Figure 4.12	Average (± 1 s.d.) concentrations of Na, K, Ca, Mg, sulfate, bicarbonate, chloride, and silica (mg/L) as a function of sampling position in gate 1 at the Denver Federal Center	65
Figure 4.13	Average (± 1 s.d.) concentrations of Na, K, Ca, Mg, sulfate, bicarbonate, chloride, and silica (mg/L) as a function of sampling position in gate 2 at the Denver Federal Center	66
Figure 4.14	Average (± 1 s.d.) concentrations of Na, K, Ca, Mg, sulfate, bicarbonate, chloride, and silica (mg/L) as a function of sampling position in gate 3 at the Denver Federal Center	67
Figure 4.15	Picture showing cemented nodules recovered from core collected at the Denver Federal Center	69
Figure 4.16	Picture showing the appearance of cores collected at the Denver Federal Center, from gate 2 near the upgradient peagravel/iron interface	69
Figure 4.17	Concentration distribution of solid phase inorganic carbon in angle cores collected from gate 1 at the Denver Federal Center	72
Figure 4.18	Concentration distribution of solid phase inorganic carbon in angle cores collected from gate 2 at the Denver Federal Center	72

Figure 4.19 Concentration distribution of solid phase inorganic carbon in a vertical core collected from gate 2 at the Denver Federal Center	73
Figure 4.20 Concentration distribution of solid phase sulfur in angle cores collected from gate 1 at the Denver Federal Center	73
Figure 4.21 Concentration distribution of solid phase sulfur in angle cores collected from gate 2 at the Denver Federal Center	74
Figure 4.22 Inorganic carbon concentrations versus total sulfur a) Elizabeth City core materials; b) Denver Federal Center	75
Figure 4.23 Powder X-ray diffraction data from fine-grained materials removed via sonication from cores collected at the Denver Federal Center PRB (core C2-3-71801)	76
Figure 4.24 Scanning electron micrographs of samples from the Denver Federal Center PRB:a) sample C2-17-71300-2; b) sample C2-17-71300-7; c) sample C1-2-71000-3	77-79
Figure 4.25 Concentration of microbial biomass (from PLFA data) in picomoles per gram in iron from near the upgradient peagravel/iron interface and iron from near the downgradient peagravel/iron interface: a) gate 1; b) gate 2	82
Figure 4.26 Concentration distribution of solid phase sulfur and microbial biomass (from PLFA data) in a vertical core collected from gate 2 at the Denver Federal Center (vertical cores C2-1-71901, C2-2-71901, and C2-3-71901)	83
Figure 4.27 Pie graphs showing average structural distribution of PLFA compounds in core materials from the Denver Federal Center	84
Figure 5.1 Redox –pH diagram showing composition of ground water from the Elizabeth City iron wall compared to equilibrium trends for the Fe^0 - $Fe(OH)_3$, Fe^0 - Fe_3O_4 , and Fe^{2+} - $Fe(OH)_3$ couples	88
Figure 5.2 Redox-pH diagram for the Fe - H_2O system at 25 °C, showing speciation of iron (dashed lines) and stability fields of iron-bearing minerals (solid lines).....	90
Figure 5.3 Redox-pH diagram for the Fe - CO_2 - H_2O system at 25 °C, showing speciation of iron (dashed lines) and stability fields of iron-bearing minerals (solid lines).....	90
Figure 5.4 Redox-pH diagram for the Fe - S - CO_2 - H_2O system at 25 °C, showing speciation of iron (dashed lines) and stability fields of iron-bearing minerals (solid lines).....	91
Figure 5.5 Redox-pH diagram for the Fe - S - CO_2 - H_2O system at 25 °C, showing speciation of iron (dashed lines) and stability fields of iron-bearing minerals (solid lines).....	91
Figure 5.6 Redox-pH diagram for the Fe - CO_2 - H_2O system at 25 °C, showing speciation of iron (dashed lines) and stability fields of iron-bearing minerals (solid lines).....	92

Figure 5.7	Redox-pH diagram for the Fe-CO ₂ -H ₂ O system at 25 °C, showing speciation of iron (dashed lines) and stability fields of iron-bearing minerals (solid lines).....	92
Figure 5.8	Upgradient ground-water compositions (molar ratios) and TDS values for the Elizabeth City and Denver Federal Center PRB sites	93
Figure 5.9	Comparison of total dissolved solids concentrations at PRB sites studied in the Tri-Agency initiative	93
Figure 5.10	Solubility diagram showing the stability field of carbonates as a function of pH and log activities of Ca, Fe, Mg, and dissolved inorganic carbon compared to ground-water compositions from upgradient, iron wall, and downgradient sampling locations (Elizabeth City PRB)	95
Figure 5.11	Saturation indices of magnesium-bearing phases (brucite, Mg(OH) ₂ ; sepiolite, Mg ₄ (OH) ₂ Si ₆ O ₁₅ ·H ₂ O) as a function of pH in ground water from upgradient, iron wall, and downgradient sampling locations (Elizabeth City PRB)	98
Figure 5.12	Conceptual model of the impact of mineral and biomass accumulation to PRB hydraulic performance	99
Figure 5.13	Fractional porosity reduction as a function of inorganic carbon concentration in the solid phase.	100
Figure 5.14	Fractional porosity reduction as a function of sulfur concentration in the solid phase.	102
Figure 5.15	Fractional porosity reduction as a function of the positive molar volume change as iron metal reacts to form magnetite, hematite, goethite, and ferrihydrite	102
Figure 5.16	Concentration versus time in batch tests: a) chromium; b) TCE	105
Figure 5.17	Comparison of PLFA distribution in four iron walls	107
Figure 5.18	Water levels in Elizabeth City monitoring wells	109

Tables

Table 2.1	Comparison of PRBs investigated in this study	6
Table 3.1	Contaminant concentrations in ground water upgradient of the Elizabeth City PRB	11
Table 3.2	Contaminant concentrations in ground water downgradient of the Elizabeth City PRB	12
Table 3.3	Geochemical parameters in upgradient, iron wall, and downgradient locations, Elizabeth City PRB	18
Table 3.4	Changes in concentrations of metals in transect 2 as a function of time and depth below ground surface	27
Table 3.5	Changes in concentrations of anions in transect 2 as a function of time and depth below ground surface	32
Table 3.6	Cores collected for analysis at the Elizabeth City PRB	35
Table 3.7	Results of powder X-ray diffraction analysis of core materials from the Elizabeth City PRB	41
Table 3.8	Pearson's correlation matrix of element concentrations determined by SEM-EDX analysis	46
Table 3.9	Summary of PLFA data from the Elizabeth City PRB	47
Table 4.1	Cores collected for analysis at the Denver Federal Center PRB	70
Table 4.2	Results of powder X-ray diffraction analysis of core materials from the Denver Federal Center PRB	76
Table 4.3	Results of SEM-EDX analysis of core materials from The Denver Federal Center PRB	80
Table 4.4	Summary of PLFA data from the Denver Federal Center PRB	81
Table 5.1	Mineral precipitates identified in iron walls	94
Table 5.2	Molar volume and density of mineral precipitates	101
Table 5.3	Core samples used in batch reactivity tests	103
Table 5.4	Water compositions used in batch reactivity tests	104
Table 5.5	Summary of rate data for reactions of TCE and 1,1,1-TCA with zero-valent iron (unreacted and from field PRBs)	106

Appendix A-1: Inorganic carbon and sulfur concentrations in cores collected from the Elizabeth City and Denver Federal Center PRB sites	122-126
Appendix A-2: Reduced Sulfur Speciation in Elizabeth City and Denver Federal Center Cores	127
Appendix A-3: Inorganic Carbon and Sulfur Concentrations in Denver Federal Center Cores	128-133
Appendix B-1: Phospholipid fatty-acid (PLFA) extract data from cores collected from the Elizabeth City and Denver Federal Center PRB sites	136-140

Acknowledgments

The authors would like to acknowledge all of the participants of the Tri-Agency PRB research initiative, in particular Arun Gavaskar (Battelle), Bruce Sass (Battelle), Neeraj Gupta (Battelle), Woong-Sang Yoon (Battelle), Libby West (Oak Ridge National Laboratory), Nic Korte (Oak Ridge National Laboratory), Liyuan Liang (Cardiff University), and Matt Turner (Interstate Technologies Regulatory Cooperation). Members of the Permeable Reactive Barriers Research Team contributed to the research described in this report, especially S. Acree, F. Beck, P. Clark, K. Jones, M. McNeil, C. Paul, and C. Su. Mantech Environmental Research Services Corporation provided analytical support both in the field and in the laboratory. T. Sivavec (General Electric Corporate) provided X-ray photoelectron spectroscopic analysis of iron core materials. We thank R. Ford (U.S. EPA) for many discussions throughout this study and D. Myers (East Central University) for the scanning electron microscopy. Shim Myung-Hwa, a visiting student from the Kwangju Institute of Science and Technology (South Korea), is acknowledged for her help on parts of this study. Martha Williams (CSC) provided support in document preparation. J.P. Messier (U.S. Coast Guard Support Center) is thanked for providing site assistance at the Elizabeth City site and C. Eriksson (Pacific Western Technologies, Ltd.), J. Jordon (Pacific Western Technologies, Ltd.), and M. Gasser (Pacific Western Technologies, Ltd.) are thanked for site assistance at the Denver Federal Center site. We also acknowledge the U.S. Coast Guard for access to the Elizabeth City site and the Federal Highway Administration and General Services Administration for access to the Denver Federal Center site. Reviews of the document were provided by Eric Reardon (University of Waterloo), Liyuan Liang (Cardiff University), Steve Shoemaker (Dupont), Robert Powell (Powell and Associates), Carl Eriksson (Pacific Western Technologies, Ltd.), and Thomas Holdsworth (U.S. EPA); their thoughtful comments are appreciated.